Accepted Manuscript

Accepted Manuscript (Uncorrected Proof)

Title: DCM-ML: An EEG-Based Classifier for Early Diagnosis of Schizophrenia Based on Dynamic Connectivity Matrices and Machine Learning Algorithms

Running Title: DCM-ML: An EEG-Based Classifier

Authors: Seyed Abolfazl Valizadeh¹, Marcus Cheetham², Alireza Mohammadi^{3,*}

- 1. Student Research Committee, Baqiyatallah University of Medical Sciences, Tehran, Iran.
- 2. Department of Internal Medicine, University Hospital Zurich, Zurich, Switzerland.
- 3. Neuroscience Research Center, Baqiyatallah University of Medical Sciences, Tehran, Iran.

*Corresponding Author: Alireza Mohammadi, Neuroscience Research Center, Baqiyatallah University of Medical Sciences, Tehran, Iran. Email: ar.mohammadi@bmsu.ac.ir

To appear in: Basic and Clinical Neuroscience

Received date: 2025/08/11

Revised date: 2025/09/30

Accepted date: 2025/10/8

This is a "Just Accepted" manuscript, which has been examined by the peer-review process and has been accepted for publication. A "Just Accepted" manuscript is published online shortly after its acceptance, which is prior to technical editing and formatting and author proofing. Basic and Clinical Neuroscience provides "Just Accepted" as an optional and free service which allows authors to make their results available to the research community as soon as possible after acceptance. After a manuscript has been technically edited and formatted, it will be removed from the "Just Accepted" Web site and published as a published article. Please note that technical editing may introduce minor changes to the manuscript text and/or graphics which may affect the content, and all legal disclaimers that apply to the journal pertain.

Please cite this article as:

Valizadeh, S.A., Cheetham, M., Mohammadi, A. (In Press). DCM-ML: An EEG-Based Classifier for Early Diagnosis of Schizophrenia Based on Dynamic Connectivity Matrices and Machine Learning Algorithms. Basic and Clinical Neuroscience. Just Accepted publication Jul. 10, 2025. Doi: http://dx.doi.org/10.32598/bcn.2025.2572.1

DOI: http://dx.doi.org/10.32598/bcn.2025.2572.1

ABSTRACT

Purpose: The early diagnosis of schizophrenia (SZ) continues to be challenging due to the subjective nature of clinical assessments and the heterogeneity of symptoms. There is a pressing need for objective, scalable, and non-invasive diagnostic tools to complement traditional methods. This study proposes a machine learning (ML) framework that utilizes dynamic effective connectivity matrices (DCM) derived from event-related potentials (ERP) for SZ classification.

Methods: ERP data from 81 participants, including 49 SZ patients and 32 healthy controls, sourced from a publicly accessible and anonymized dataset. Granger causality was employed to compute 64×64 directional connectivity matrices, capturing inter-electrode information flow. Feature selection through t-tests identified 2,777 significant connectivity differences (p < 0.05), which were subsequently used to train a Random Forest (RF) classifier. To address class imbalance, balanced training subsets were created. Additionally, the robustness of the model was evaluated under varying levels of white Gaussian noise (0% to 45%).

Results: The Random Forest classifier demonstrated high diagnostic accuracy (99.24%), sensitivity (98.34%), specificity (99.73%), and an F1-score of 98.91% across 100 iterations, effectively minimizing the risks of overfitting. Its performance remained robust under varying train-test splits and substantial noise levels, with an F1-score of 92% even with 45% white Gaussian noise. Feature selection significantly enhanced noise resilience and classification stability. Connectivity analysis revealed that central (Cz, FCz), occipito-parietal (PO3, Oz), and inferior (Iz) regions were key discriminators, indicating disrupted fronto-temporal and sensory integration networks in individuals with schizophrenia.

Conclusion: This study highlights the feasibility of ML-driven ERP connectivity analysis as a non-invasive tool for the early detection of SZ. Achieving near-perfect accuracy, the model demonstrates strong generalizability, interpretability, and clinical scalability, outperforming deep learning counterparts while relying on a minimal, targeted feature set. The findings underscore the diagnostic relevance of fronto-central and occipito-parietal connectivity patterns. While promising as a non-invasive diagnostic adjunct, future validation on larger, demographically diverse cohorts is essential.

Keywords: ERP, Diagnosis, Schizophrenia, Effective Connectivity, Machine Learning, Classification.

Introduction

Schizophrenia (SZ) is a chronic mental disorder with a polygenic basis and an 80% heritability rate. It is characterized by symptoms such as hallucinations, delusions, disorganized behavior, and progressive cognitive impairments (1). It affects approximately 20 million people worldwide (2). Early diagnosis and intervention can significantly impact the lives of affected individuals. Early diagnosis allows for prompt intervention of psychotic symptoms (e.g., hallucinations, delusions, and disorganized thinking) before they become more severe, improves outcomes and long-term prognosis (e.g., daily-life functioning, stability in social, academic, or work life), and prevents or delays relapses and lessens the likelihood of hospital admissions (3–6). Early diagnosis can also help to lessen the disabling aspects of the disorder (e.g., cognitive impairments or social isolation) and improve the quality of life for patients and family (7).

While timely detection of schizophrenia is crucial, detection is heavily reliant on manual evaluation during clinical assessment (8). This conventional approach to clinical diagnosis is challenging due to the high heterogeneity of SZ (9). SZ can manifest differently across individual patients and throughout the disease, with some patients predominantly presenting positive and others negative and cognitive symptoms (10). SZ can also show symptom overlap with other psychiatric disorders (e.g., depression), making differential diagnosis difficult without a comprehensive understanding of the patient's medical history (10). The subjective nature of manual evaluation is prone to human error and time-consuming (11).

Symptom onset in SZ typically occurs during adolescence and early adulthood (between 14 and 30). The time between symptom onset and diagnosis and treatment is consistently found to be one of the best predictors of later prognosis (12). The prodromal stage, during which initial symptoms may manifest, is a critical period for identifying and intervening in the progression of SZ. is While cognitive symptoms can be apparent even before this stage, detecting them for diagnostic purposes is especially challenging due

to their ambiguity, as they are often mild or nonspecific.

When symptoms are ambiguous, individuals at risk of schizophrenia may show irregularities in resting-state and task-related EEG activity (13,14). These can include alterations in the temporal dynamics, coordination and functional connectivity between different brain regions (e.g., instability in dynamic functional connectivity, hypo- and hyper-connectivity) compared to healthy individuals (15–19). Altered brain activity patterns might provide valuable insights into the likelihood of developing schizophrenia.

We explored the feasibility of a novel approach to EEG dynamic analysis based on estimates of functional or effective brain connectivity in combination with machine learning (ML) techniques and algorithms to aid early diagnosis of SZ. The rationale for applying EEG Dynamic Analysis for SZ detection is that SZ many be considered as a disorder of brain network organization (20). In the present study, we re-applied a novel feature extraction approach called Dynamic Connectivity Matrices (DCM) and utilized the generated features in combination with an ML algorithm that was previously developed to identify based on their unique patterns of dynamic functional connectivity in EEG (21). Standard EEG data were acquired from a clinically well-characterized cohort of adult patients. Using Electroencephalography (EEG) and Event Related Potential (ERP) data, the expectation was that this approach to EEG dynamic analysis would accurately distinguish individuals with schizophrenia from those without. To inform further development of this approach, we asked which combination of metrics is most informative for accurately classifying SZ. Evaluation criteria were the accuracy, sensitivity and specificity of ML-based classification of clinically diagnosed SZ patients and healthy individuals.

Methods

Dataset and Participants

We conducted a retrospective analysis of EEG data from N=81 participants sourced from a publicly accessible and anonymized dataset (https://www.kaggle.com/datasets/broach/ button-tone-sz). The EEG dataset

used in this study was obtained from a publicly available source (www.kaggle.com). According to the dataset description, informed consent had already been obtained from all participants for further use, and the data was fully anonymized. Therefore, no additional ethical approval or consent was required for its use in this study. However, all methods and analyses were conducted in accordance with the relevant guidelines and regulations, and the study protocol was approved by the Research Ethics Committee of Baqiyatallah University of Medical Sciences (Ethics code: IR.BMSU.BAQ.REC.1403.147). This dataset includes EEG signals acquired from n=49 SZ patients (41 male, between 22 and 63 years, M= 40.0; SD=13.5) (17 in early stages and 32 in chronic stages of the disorder) and n= 32 healthy controls (26 male, between 22 and 63 years, M= 38.2; SD=13.0). Data was acquired while participants performed a passive (auditory-only) condition of a basic auditory listening task. All patients were clinically diagnosed using Structured Clinical Interview for DSM-IV (SCID). Patients and healthy controls had no other diagnoses.

Data acquisition

EEG data were captured with a 64-channel Active Two Biosemi system (22) and cap, following the 10-10 international system, while participants engaged in the auditory listening task. This task entailed the presentation of 100 auditory stimuli (1000 Hz tones at 80 dB SPL for a duration of 50 ms.) with inter-stimulus intervals (ISIs) varying between 1000 and 2000 milliseconds. EEG signals were recorded continuously and divided into separate ERP epochs of 3000 ms. Those were synchronized with the onset of each tone. The dataset also includes data acquired from an auditory-motor task (23,24) that were not used in the present study. The data were collected at a sampling frequency of 1024 Hz and down sampled to 512 Hz.

EEG Preprocessing and Epoching

The EEG dataset was originally preprocessed and cleaned for a previously published study (23,25) and further processed and cleaned by the same

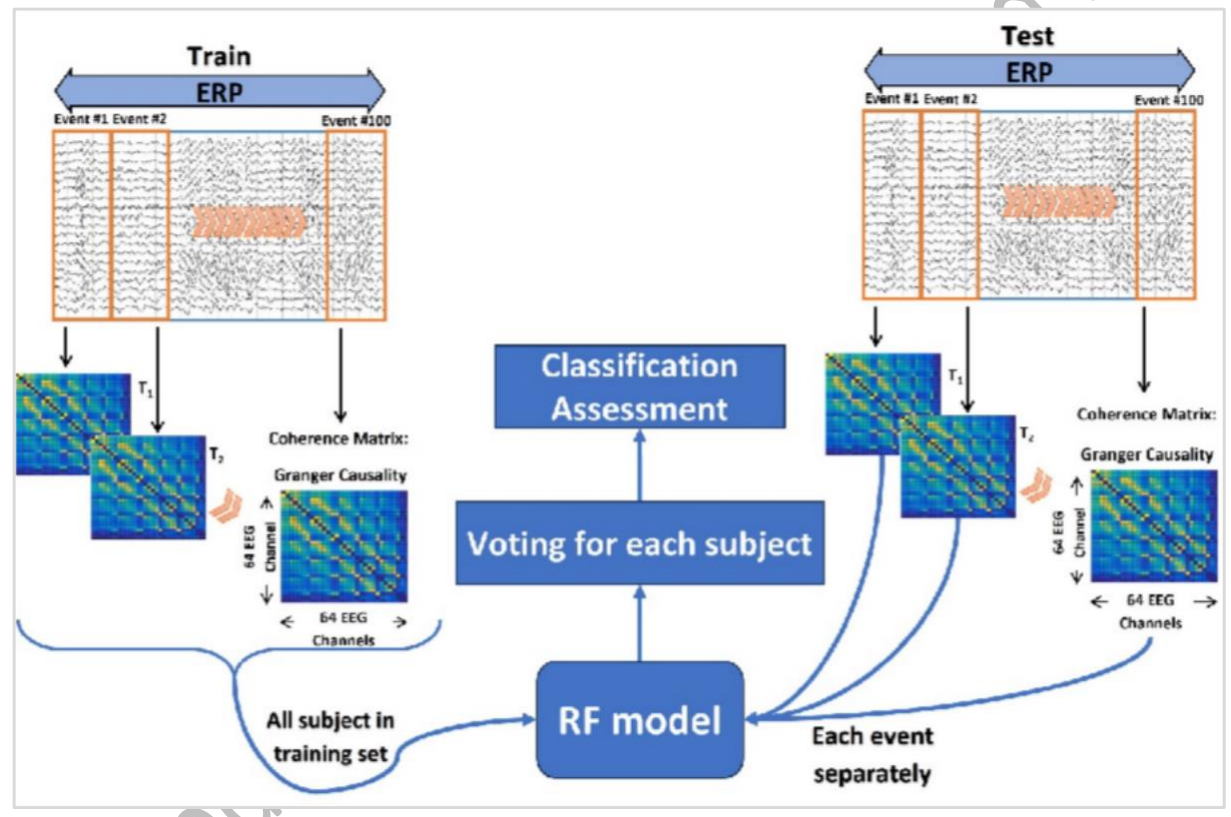
authors prior to public release. Utilizing a publicly available dataset promotes research transparency, facilitates reproducibility, and supports further investigation by other researchers.

The preprocessing steps included re-referencing to averaged earlobe electrodes, band-pass filtering between 0.5 and 15 Hz, and Independent Component Analysis (ICA) for the identification and removal of ocular and muscular artifacts. A regression-based algorithm was applied to correct for eye movement and blink activity across all scalp channels. Artifact rejection was performed using a $\pm 100~\mu V$ threshold at each electrode, and non-physiological channels were interpolated based on established spatial criteria. These procedures ensured high-quality, artifact-free EEG data suitable for connectivity analysis.

For this study, the preprocessed EEG signals were segmented into 3000-ms epochs, each time-locked to the onset of the auditory stimulus. Baseline correction was applied using the window beginning 600 ms to 500 ms before tone onset.

Signal processing and epochs

Unlike traditional ERP analysis, which relies on averaging epochs to extract features, our approach treated each epoch as an independent sample. This single-trial analysis significantly expanded the dataset size, enabling the model to capture subtle inter-trial variability in neural activity. This is advantageous for studying complex neurological disorders like SZ, where subtle differences in neural responses may be obscured by averaging. By analyzing each epoch individually, finer-grained neural patterns were sought in line with recent



advancements that emphasize the importance of trial-to-trial variability for capturing brain function²⁷⁻²⁹.

Fig. 1. Time-domain EEG connectivity analysis using coherence Granger causality for ERP classification. The epochs were 3000 milliseconds (ms) in length and time-locked to the onset of the auditory stimulus (i.e., the tone). Granger causality was computed for the 3000-ms epoch and created 64*64 matrices for each epoch. The workflow illustrates the processing of cleaning the EEG data and epoching it into stable segments representing Event-Related Potentials (ERPs) for both training and testing. Coherence Granger causality was applied to each epoch to assess directional information flow between 64 EEG electrodes in the time domain, producing a 64x64 coherence matrix indicative of pairwise electrode connectivity. These matrices served as features for a Random Forest (RF) classifier. Classification assessment involved a voting process across participants, trained on the training participants and evaluated on each event

in test participant separately. Feature extractor

Our classification framework is based on a novel and previously validated subject identification method (21). This method uses surface-level (electrode-based) functional connectivity in the time domain, computed over short, overlapping temporal windows, and generates Temporal Dynamic Connectivity Matrices (TDCMs), which capture the evolving patterns of interaction between EEG electrodes. Within each temporal window, the statistical relationship - whether correlational or causal - is quantified between pairs of EEG time series. This dynamic representation enables fine-grained tracking of brain network changes over time and has been adapted in the present study to serve as input features for classifying SZ-related neural activity.

The clean EEG data were divided into epochs, each deemed sufficiently stable for connectivity analysis. Within each epoch, coherence Granger causality was used to assess interactions between EEG signals from different electrodes in the time domain (see Figure 1). Causation, or directional connectivity, was used to evaluate how much activity in one EEG electrode could predict activity in another. All analyses were performed in the time domain, with the exception of the initial filtering stage. An iterative method was employed to determine the interaction between each seed electrode and every other electrode, producing a 64x64 matrix that illustrates the pairwise connectivity among all electrode pairs.

Granger causality is a statistical method used to assess whether one timeseries can predict another. If past values of variable X significantly improve the prediction of variable Y— beyond what is possible using Y's own history—X is said to "Granger-cause" Y. This is typically evaluated using a linear regression model, where the target time series is regressed on its own past values and those of another series; statistical significance of the latter indicates predictive influence.

In EEG analysis, Granger causality is applied to identify directional interactions between brain regions, providing insight into neural connectivity associated with cognitive processes and disorders such as SZ (26,27). Importantly, Granger causality reflects predictive, not necessarily direct, causal

relationships, suggesting information flow from electrode to another.

Granger Causality is computed as follows:

- 1. Model Specification:
 - Two time-series, X and Y, are examined.
 - A regression model is constructed for Y based on its previous values in conjunction with the past values of Y.

2. Lag Selection:

 Identify the appropriate lags for the time series. This can be achieved through metrics like the Akaike Information Criterion (AIC) or the Bayesian Information Criterion (BIC).

3. Regression Analysis:

- Conduct two regression analyses:
- Model 1:

$$Y_t = a_0 + a_1 Y_{t-1} + a_2 Y_{t-2} + \dots + a_n Y_{t-n}$$

Model 2: Model 2 includes past values of X.

$$Y_t = a_0 + a_1 Y_{t-1} + a_2 Y_{t-2} + \dots + a_n Y_{t-n} + c_1 X_{t-1} + c_2 X_{t-2} + \dots + c_n X_{t-n}$$

4. Hypothesis Testing:

- The null hypothesis H_0 posits that X does not Granger-cause Y (i.e., the coefficients

$$c_1,c_2,...$$
 are equal to zero).

- Implement an F-test to juxtapose the two models. Should the inclusion of X substantively enhance the predictive capacity for Y, the null hypothesis is rejected, indicating that X Granger-causes Y.

To ensure consistency and avoid model complexity or potential overfitting, we did not perform individual model selection using information criteria such as BIC or AIC. Instead, we set the model lag order to a fixed value of 10 across all participants and conditions. This approach simplifies the analysis pipeline and ensures cross-subject comparability while remaining within the range generally adequate to capture relevant temporal dependencies in EEG time series data.

Machine learning procedures

The number of participants in each group is unbalanced, with 32 healthy individuals and 49 individuals with schizophrenia. To prevent unbalanced learning, we used the HC sample, chose half for training, and picked an equal number of participants from the schizophrenia group. This led to 16 participants chosen at random from each group for training. We subsequently categorized the remaining healthy participants and individuals with schizophrenia. This approach reduces the classifier's performance but improves its dependability for evaluating each extra participant. The classifiers are fed directly by the connectivity matrices. Every training step, along with the classifiers, was performed on the training set. The number of epochs for each participant remains the same.

To mitigate the potential for overfitting, a particular concern in smaller datasets with k- fold cross-validation, we employed a 50/50 train-test split. This approach aimed to maximize data utilization while minimizing overfitting risk. Prior to classification, a feature selection phase was conducted to refine the feature space and potentially enhance model performance. Independent two-sample t-tests were performed on the training datasets to identify connectivity features exhibiting statistically significant differences (p < 0.05) between the defined groups: healthy controls and individuals with SZ. Only these features were retained AS input features for the classification algorithms.

This feature selection approach was designed to reduce dimensionality, minimize noise and improve model performance by focusing on the most salient and discriminatory features. This enhances the model's ability to accurately categorize individuals into their respective diagnostic groups and the interpretability of the model by highlighting neural connectivity patterns associated with SZ.

The feature set comprised 64*64*100 epochs, indicating that each participant contributed 100 samples, each with 64*64 features. Consequently, the training set for each class consisted of 16*100 samples, each with 1*4096 elements (i.e., a 1×4096 feature vector). The final training set was structured as

a matrix with 3200 rows (samples) and 4096 columns (connections). An additional column was appended to the data as the class label, indicating group membership (SZ or non-SZ). A t-test was conducted based on this class label. The classification of each epoch within the test set was performed independently. A participant was classified as SZ if a majority of epochs (at least 51 out of 100) were labeled as SZ; otherwise, they were classified as non-SZ.

Classification

The classification process was performed on all test epochs. The classification set was determined according to the following criteria: Participants were labeled SZ or non-SZ based on the majority classification of their epochs. Those with an equal number of SZ and non-SZ epochs would have been designated as unknown; however, no participants fell into this category in the current dataset.

Classifier

The RF algorithm (28) is a robust machine learning algorithm and particularly effective for classification tasks, including medical diagnosis prediction. It operates by constructing an ensemble of decision trees, each trained on a random subset of the data. This bootstrapping approach ensures that each tree learns diverse aspects of the data, mitigating overfitting and improving generalization. In predicting, every tree in the forest votes, and the most common class or the average prediction is selected as the result. This collective characteristic provides multiple benefits (21):

- Great Precision: The combined knowledge of several trees frequently results in very precise predictions.
- Resilience to Noise: The algorithm remains strong against noisy data and outliers because of the ensemble's averaging impact.
- Evaluation of Feature Importance: Random Forest offers insights into the significance of various features, assisting in feature selection and aiding in comprehending the fundamental patterns present in the data.

- Managing Absent Data: It efficiently manages absent data in the dataset.
- Scalability: Random Forest effectively manages extensive datasets,
 rendering it appropriate for practical applications.

Classification Assessment

Accuracy assesses the overall correctness of a model's predictions, indicating the ratio of correctly classified cases to the total instances. Although high accuracy often suggests strong performance, it can be deceptive in imbalanced datasets where one class greatly exceeds the other. Sensitivity, referred to as recall, evaluates the model's capacity to accurately identify positive cases, which is essential when the penalty for failing to detect a positive instance is significant. On the other hand, specificity evaluates the model's capacity to accurately recognize negative instances, which is essential when the misclassification of a negative instance can lead to serious outcomes. The F1-score, which is the harmonic mean of precision and recall, offers a single measurement that balances both factors, especially useful in imbalanced datasets.

Selecting the appropriate metric relates to accurately detecting both positive and negative cases. Note that there is frequently a compromise between sensitivity and specificity;

enhancing one usually results in a decline of the other. In addition, accuracy may be misleading in imbalanced datasets, as metrics such as sensitivity, specificity, and F1-score provide a more nuanced assessment of model effectiveness.

An additional strategy was implemented to evaluate the robustness of the classification outcomes. This strategy relates to the following consideration. if a neural network is trained to recognize stimuli, its performance should remain consistent when identifying stimuli, like faces, from various angles, under differing lighting conditions, or when presented with partial facial features (21,29). This means that the classifier must retain accuracy even when target stimuli are altered or degraded. To replicate such scenarios, white Gaussian noise was incrementally introduced into the test dataset's connectivity matrices. Initially, the classification analysis was conducted without noise (0% noise level). Subsequently, noise was linearly added to all features in increasing increments, starting at 5% and progressing to 45%. This process resulted in nine distinct ten conditions (0%, 5%, 10%, 15%, ..., 45%), each subjected to separate classification evaluations.

Results

The RF model showed very high overall performance through various assessment metrics, evaluated over 100 iterations to reduce the impact of overfitting and random effects (see Table 1). Sensitivity, a metric reflecting the model's ability to correctly identify positive instances, reached 0.98, with a confidence interval of 98.34±0.04%. This indicates that the model was highly accurate in detecting the target condition when it was present. Similarly, specificity, which evaluates the model's ability to correctly identify negative instances, achieved a perfect score of 1.00 with a confidence interval of 99.73±0.01%, demonstrating that the model did not mislabel any negative cases. The F1 score, balancing precision and recall, was also high at 0.99 with a confidence interval of 98.91±0.02%, emphasizing the model's strong predictive capacity. Finally, the overall accuracy of the model, determined by the proportion of accurate predictions, was 0.99 with a confidence interval of

99.24±0.02%, indicating that the model generated highly accurate predictions on the dataset.

Table 1. Overall result for 100 runs.

Feature	Metrics	Mean	Standard	Confidence Interval	Confidence Interval
Selection			Deviation	Lower	Upper
All features	Sensitivity	67.78%	1.79%	67.42%	68.14%
	Specificity	98.73%	0.29%	98.67%	98.73%
	F1 Score	87.67%	0.79%	86.88%	87.22%
	Accuracy	87.05	0.86%	87.51%	87.84%
Selected Feature	Sensitivity	98.34%	0.16%	98.30%	98.38%
	Specificity	99.73%	0.05%	99.72%	99.74%
	F1 Score	98.91%	0.10%	98.89%	98.93%
	Accuracy	99.24%	0.07%	99.23%	99.26%

Test Train Rate

Figure 2 demonstrates the impact of the test rate on classification performance. Notably, the RF classifier shows very high performance even with relatively limited training sample sizes. This is consistent with previous studies that highlighted the effectiveness of RF classifiers in handling imbalanced datasets and their ability to generalize well to unseen data (30). However, when the testing rate approaches very high values (0.09 and 0.95), a decline in classification accuracy is observed. This trend shows that while RF classifiers are generally robust against data distribution, significant imbalances can still negatively influence their performance. This finding aligns with current research, suggesting that imbalanced datasets can pose challenges for ML models, potentially leading to biased results. To confirm that the observed performance trends were not a result of random factors, we methodically adjusted the test rate from 5% to 95% of the overall epochs (see Table 2). This method enabled us to evaluate the classifier's strength across various data distributions. Despite a test rate of 95%, the RF classifier obtained an F1-score of 92%, indicating its capability in managing imbalanced datasets.



Fig. 2. Impact of the test/train rate on classification performance.

Table 2. Impact of different test/train rates on Random Forrest classification performance.

Noise stability

Figure 3 illustrates how rising levels of white Gaussian noise affect the classification performance of two sets of features: "All Features" and "Selected Features Noise was progressively introduced to the connectivity matrices of the test dataset, simulating scenarios in which target stimuli are modified or compromised. The x-axis represents the percentage of introduced noise, ranging from 0% (no noise) to 45%, while the y-axis displays the F1-score, a metric that quantifies classification accuracy. As the percentage of noise increases, both feature sets exhibit a decline in F1-score, indicating a reduction in classification effectiveness. However, the "Selected Features" (blue line) demonstrate greater resilience to noise, consistently achieving a higher F1-score than the "All Features" set (red line) across all noise levels. This suggests that the "Selected Features" are more robust against the detrimental effects of noise and provide more reliable classification, even when the data is compromised.

F1-Score Trend with Added Noise

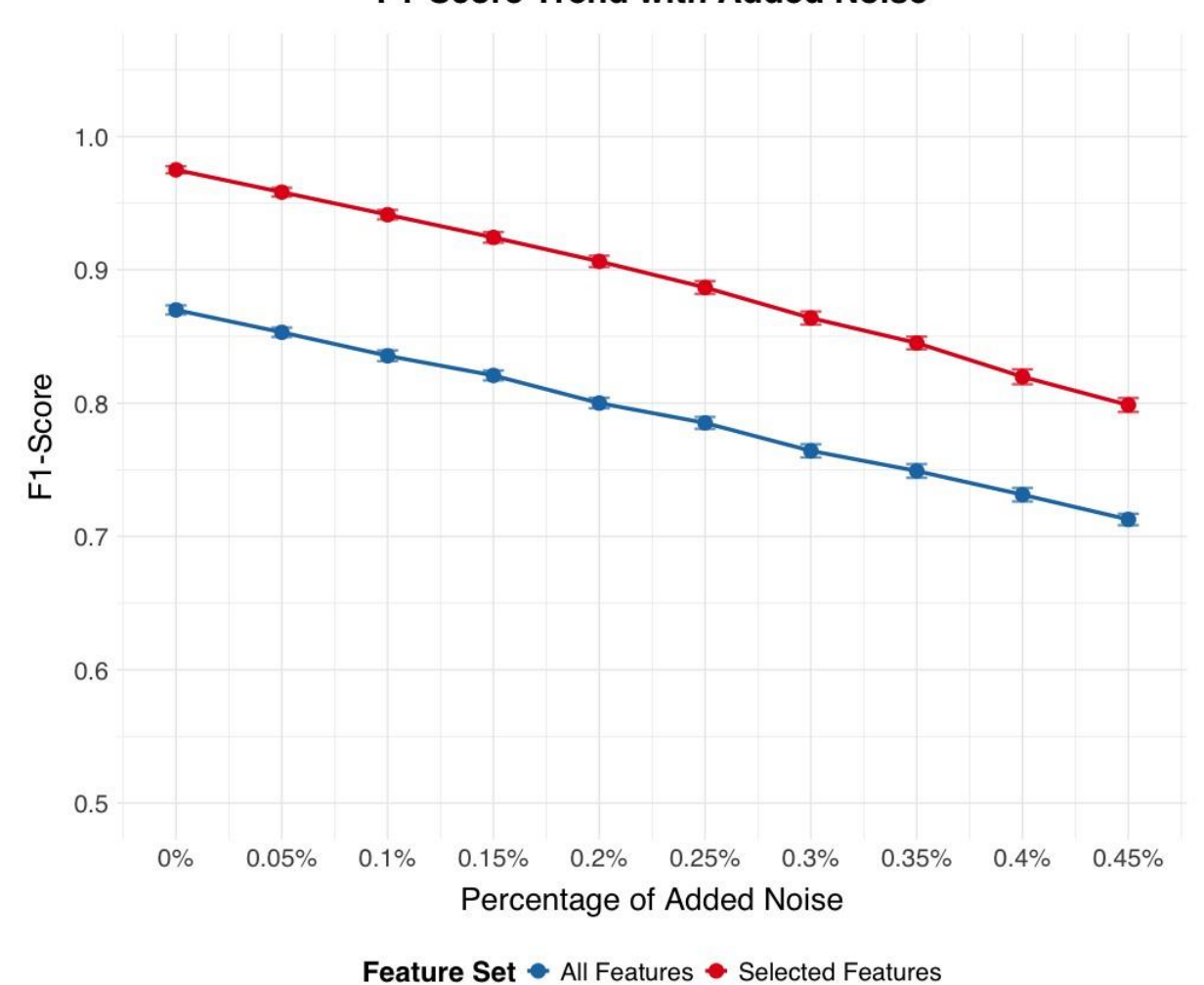


Fig. 3. Noise stability and classification performance. This figure illustrates for all (blue line) and selected features (red line) the percentage of added noise, ranging from 0% (no noise) to 45% on the x-axis against the F1-score (i.e., classification accuracy) on the y-axis. Error bars represent confidence intervals of the F1-score calculated over 100 runs or folds.

VCC6.bic,

Electrode contribution to classification

Through a comprehensive analysis of Granger causality across all 64x64 electrode pair combinations, we identified 2,777 connections that exhibited statistically significant differences between the healthy control (HC) and SZ groups (p-values ranging from 0.049 to 10^{-74}) on the basis of trained datasets. Table 3 presents the most discriminatory Granger causality combinations, characterized by particularly robust statistical significance (p < 10^{-30}). To further investigate the regional brain areas most implicated in these group differences, we created a frequency table. This table is based on all Granger causality combinations that demonstrate significant group separation (p < 0.05), and counts how often each electrode appears as either a predictor or a predicted region across these significant connections. The most frequently identified electrodes through this process will be presented in a subsequent table, aiming to highlight key regions involved in connectivity alterations related to schizophrenia.

Table 3. Granger causality combinations that significantly differentiate the healthy and SZ groups (E = Power of ten).

#	Independent	Dependent	P-Value	#	Independent	Dependent	P-Value
1	PO3	Cz	4.61E-74	20	P7	FC3	1.05E-33
2	Fz	Cz	5.81E-55	21	PO7	C1	1.82E-33
3	TP7	PO3	2.24E-54	22	Oz	TP10	5.76E-33
4	PO3	FCz	7.41E-54	23	P7	C1	7.30E-33
5	TP7	C1	8.85E-51	24	C1	CP3	1.01E-32
6	T7	PO3	3.04E-48	25	PO3	FC3	2.33E-32
7	C5	PO3	3.41E-45	26	T7	C1	6.63E-32
8	PO3	FC1	6.17E-43	27	Fz	PO3	6.95E-32
9	P3	FC1	4.51E-41	28	Oz	C2	7.05E-32
10	FC5	PO3	1.00E-40	29	lz	FCz	1.82E-31
11	P3	Cz	2.67E-40	30	Oz	FC2	4.72E-31
12	PO3	C2	2.98E-39	31	Cz	CP4	4.96E-31
13	C3	POz	1.36E-37	32	P5	FC1	5.46E-31
14	Oz	Cz	1.34E-35	33	P4	P2	1.50E-30
15	AF3	FC5	4.70E-35	34	Fz	FCz	2.99E-30
16	01	C2	1.35E-34	35	PO3	FC2	3.77E-30
17	01	FCz	2.14E-34	36	POz	FCz	3.87E-30
18	P3	FCz	3.70E-34	37	AF3	F5	6.32E-30
19	PO7	FCz	1.00E-33	38	Cz	CP3	7.04E-30
19 PO7 FC2 1.00E-33 38 C2 CP3 7.04E-30							
C							

Following the identification of the 2,777 statistically significant Granger causality combinations that differentiated the healthy control and schizophrenia groups (p < 0.05), a frequency analysis was performed to determine the most relevant electrode regions (see Table 4). This table reports the top ten electrodes ranked by their total frequency of appearance in these significant connections. For each electrode (column 1), the table shows its frequency as a predictor electrode (column 2), its frequency as a predicted electrode (column 3), and the summed total frequency (column 4). Higher total frequency indicates greater involvement in group-discriminating Granger causality relationships.

Table 4. Frequency of electrode involvement in significant Granger causality differences.

Electrode name	Predictor	Predicted
Cz	51	58
FCz	47	59
lz	50	55
PO3	49	55
CP4	42	61
AF3	47	54
C1	45	56
01	48	53
POz	54	46

Discussion

The present study was guided by two primary research questions: Is it possible to identify SZ using our novel EEG-based ML classifier based on DCM, and which combination of metrics is most informative for classifying SZ? The DCM-ML approach identified SZ to a very high degree of accuracy that approached 100%. Our findings indicate that only a subset of metrics is required to achieve effective classification of individual participants, highlighting the efficiency and specificity of the selected features. These results

underscore the potential of using targeted metrics to enhance the precision of SZ detection.

The RF model demonstrated very high performance across various metrics. It achieved a sensitivity of 0.98 (98.34% \pm 0.04%), indicating its proficiency in accurately identifying positive cases. In addition, it exhibited a perfect specificity of 1.00 (99.73% \pm 0.01%), demonstrating its performance in correctly classify negative instances without mislabeling. The model also achieved a high F1 score of 0.99 (98.91% \pm 0.02%), indicating a strong balance between precision and recall. Furthermore, the overall accuracy was 0.99 (99.24% \pm 0.02%), which is consistent with the model's ability to generate highly accurate predictions on the dataset. These results underscore the potential of targeted metrics in enhancing the precision of schizophrenia diagnosis.

The study also assessed the stability of the proposed classification method under different conditions. The introduction of white Gaussian noise led to a gradual, but predictable, decline in classification performance. Up to a noise level of 10% of the data, the accuracy remained above 95%, demonstrating considerable resilience. However, beyond 10%, the accuracy decreased more rapidly, highlighting the sensitivity of ERP-based connectivity measures to excessive noise. This underscores the importance of stringent data acquisition protocols and noise reduction techniques in ERP studies.

The RF classifier exhibited strong performance across different training sample sizes, demonstrating its ability to generalize effectively even with limited data. This finding is consistent with prior research, which has emphasized the robustness of RF classifiers in handling imbalanced datasets and their capacity to maintain high accuracy under constrained conditions. However, when the testing rate approached extreme values (0.09 and 0.95), a decline in classification accuracy was observed. This suggests that while RF classifiers are generally resilient to variations in data distribution, significant imbalances can still adversely affect their performance (21,29,31–33).

Our findings on the specific ERP components and inter-electrode connectivity patterns offer valuable insights into the neurophysiological

underpinnings of SZ. Notably, our analysis revealed that a subset of electrodes—Cz, FCz, Iz, PO3, CP4, AF3, C1, O1, and POz—were particularly influential in distinguishing individuals with schizophrenia from healthy controls. This emphasis on a targeted set of electrodes strikes a balance between diagnostic accuracy and the practical considerations of clinical EEG procedures.

The prominence of central midline electrodes, particularly Cz and FCz, in our findings aligns with existing literature that emphasizes the role of these regions in SZ pathophysiology. As highlighted in the literature, Cz is consistently identified as a core component in optimal electrode subsets for schizophrenia detection, likely due to its sensitivity to global neural dynamics and altered connectivity patterns in resting-state paradigms (34,35). The involvement of FCz, while sometimes represented by the functionally proximal Fz in standard montages, further supports the importance of frontocentral activity in capturing auditory- evoked anomalies and deficits related to auditory steady-state responses (ASSR) in schizophrenia (36). These findings suggest that disruptions in information processing and sensory integration, often observed in SZ, are reflected in the altered activity and connectivity of these central and frontocentral regions.

The present study also identified other key electrodes, including those in occipital (O1, POz), parietal (CP4), and frontal (AF3) regions, as contributing to accurate classification. The involvement of O1 aligns with evidence of visual processing abnormalities and default mode network disruptions in schizophrenia (34,37). While POz, CP4, and AF3 may not have been as extensively studied in classification frameworks, their inclusion in our model and their presence in network analyses suggest their potential role in capturing specific aspects of the disorder, such as visuospatial integration deficits (POz), right-lateralized connectivity abnormalities (CP4), and prefrontal cortex dysfunction (AF3). The inclusion of C1, near the primary somatosensory cortex, points towards possible sensorimotor integration abnormalities in SZ, though further research is needed to validate its specific contribution to classification models. The relative lack of direct evidence for Iz in the literature 40 suggests its

limited diagnostic value within current paradigms. Taken together, these results indicate that a distributed network of brain regions, extending beyond the frontal cortex, contributes to the neurophysiological signature of schizophrenia.

Imbalanced datasets pose challenges in machine learning. The present results align with existing literature in this regard⁴¹. The observed decline in accuracy at very high testing rates highlights the potential for biased outcomes when data distributions are significantly skewed. This emphasizes the need for careful consideration of dataset composition and the application of strategies to mitigate the effects of imbalance, such as resampling techniques or algorithmic adjustments, to ensure the reliability and generalizability of classification models.

Comparison of the model with other models

The dataset used in this study has been previously analyzed, using both traditional machine learning algorithms (38–40) and recent deep learning methods (41–45). These studies have established performance benchmarks and demonstrated the dataset's value for detecting neuropsychiatric disorders like SZ.

Although deep learning techniques have achieved high accuracy (up to 97%), their complexity, large model sizes, and high computational demands often limit their applicability in time-sensitive, real-world clinical settings.

To address this limitation, this present study presents a novel, computationally efficient machine learning model applied to the same dataset. This approach achieves an extremely high classification accuracy (99.24%, 98.34%, 99.73%) with no need for deep hierarchical networks or dense feature engineering. Extracting ERPs from a cognitive auditory task, we observe task-related brain dynamics and construct directional DCMs according to Granger causality. This approach also accurately maps inter-electrode information flow while preserving single-trial variability —an essential dimension usually lost to average-based or resting-state methods.

Compared to existing work, our approach displays several distinctive

advantages. For instance, Chen et al (46). use resting-state EEG and dynamic functional connectivity to achieve multi-class classification of various psychiatric disorders with moderate accuracy (73.1%). However, their method is based on averaged DFC states and does not account for signal variability or noise resistance. Our method, by contrast, relies on single-trial ERP data, retaining inter-epoch variability and exhibiting significant robustness to noise with an F1- score of 92% even in the presence of 45% Gaussian noise—a point fully unexplored in their work.

Similarly, Shen et al. (47) employ cross-mutual information in the alpha band and a 3D CNN for SZ discrimination from resting-state EEG with 97.74% accuracy. Their approach is effective but relies on undirected, frequency-specific connectivity rather than the temporal specificity our ERP-based paradigm enables. Our model not only leads to better accuracy but also offers greater interpretability and clinical utility through the selection of directionality patterns of connectivity and electrode-level biomarkers, particularly in fronto-central and occipito-parietal regions that are critical to SZ pathology.

A further recent paper (48)utilising Symbolic Transfer Entropy (STE) on resting-state EEG also has high performance (96.92%) with minimal features. In the absence of task engagement, however, their approach may lose critical neurocognitive signatures of SZ. Our DCM-based model, with direction-aware task-evoked P300 responses, can extract functional impairments in challenging cognitive conditions and is facilitated by direction-aware DCMs, offering a more comprehensive description of inter-regional interactions. Again, our model's noise resistance and ability to maintain subtle pathological signals through single-trial analysis position it as a more clinically viable instrument.

Table 5: Comparative Summary of Studies Using the Button-Tone-SZ Dataset

Study/Year	Model & Features	Performance
Al Mazroa, 2025 [49]	Cascaded Atrous Conv. Network (CA-AWFM); multi- scale adaptive fusion	99.5% accuracy
Barros[25]	Deep CNN (SzNet), single-trial ERP, 5 midline electrodes (Fz, FCz, Cz, CPz, Pz)	78% accuracy
Shaffi, Rani, Srinivasan, Huang [27,38–40]	CNNs, classical ML (RF, SVM, LDA)	Variable (75–85%)
Shen [47]	Cross-mutual information in the alpha band and a 3D CNN	97.44% accuracy
Chen[46].	resting-state EEG and dynamic functional connectivity	73.1% accuracy

Compared to a range of recent studies that have employed both deep learning and classical machine learning techniques for SZ detection using EEG or ERP data, the present study offers a unique combination of interpretability, robustness, and clinical relevance. While several approaches report high classification accuracies — for example, 99.5% using a Cascaded Atrous Convolutional Network (CA-AWFM)(49) with multi-scale feature fusion and 99.9% via ERP feature integration and demographics — these methods often rely on black- box architectures or require multimodal data inputs, which can limit clinical transparency and scalability. In contrast, our study achieves comparably high accuracy (99.24%) using a single- modality ERP dataset and a RF classifier trained on features derived from directional DCMs computed with Granger causality. This approach emphasizes inter-regional information flow, a critical neural marker often overlooked in frequency-domain or undirected methods.

While methods like SchizoGoogLeNet and Multiple Kernel Learning (MKL) also achieve strong results (50,51), they typically depend on either large-scale automated feature extraction or fusion of multiple ERP components (e.g., P300, MMN), requiring extensive preprocessing pipelines. Our model, by

contrast, is noise-resilient—maintaining a 92% F1- score even under 45% added Gaussian noise—and uses single-trial data to preserve the subtle inter-epoch variability vital for identifying schizophrenia-related deficits. In addition, our identification of clinically relevant electrode-level patterns in fronto-central and occipito- parietal regions makes the findings more explainable and suitable for integration into real- time or portable diagnostic tools.

While deep learning models such as those of Mazroa et al. (49) demonstrate impressive levels of accuracy, their complexity, limited interpretability and reliance on resting-state signals or black-box convolutional layers hinder real-world deployment. In contrast, our method balances accuracy, interpretability, and practicality, making it a well-suited for scalable clinical translation — especially for early SZ detection in settings with limited computational resources and variable signal quality.

In summary, the present approach overcomes limitations of existing methods by combining interpretable directionality features with a high-performance yet lightweight classifier to a practical, scalable, and highly accurate means to early SZ diagnosis.

This approach has the potential to bridge algorithmic performance with real-world clinical usability.

Limitations and future work

From a clinical perspective, this approach shows promise as a complementary tool for early diagnosis of SZ. At this stage, our study serves as a proof-of-concept of our ML-approach and the results should be interpreted in terms of feasibility of this ML-based classifier for clinical application. The findings suggest that the ML-based classifier may detect early-phase EEG abnormalities associated with SZ. s. However, predictive models must also account for the variability in individual disease progression. Additionally, the current dataset does not allow for an assessment of whether these abnormalities overlap with other mental health conditions. Future development of the current approach should consider disease progression and comorbidities within a demographically and clinically broader and more diverse

dataset than that used in this study to verify the method's reliability and clinical applicability. This could be supported by acquiring longitudinal data to identify consistent patterns of EEG abnormalities (and changes in these patterns) prior to the prodromal phase, throughout the prodromal transition, and after the onset of psychosis. Such data could serve as a foundation for developing reliable predictive markers. Although the high accuracy of the model is promising, understanding the specific features or patterns that influence the predictions is crucial. Integrating this approach with multimodal data (e.g., biomarkers and clinical evaluations) may enhance diagnostic accuracy. Further efforts to improve the model's interpretability will be essential for its integration into clinical practice.

Conclusion

The tested approach using a novel EEG-based classifier based on dynamic connectivity matrices and machine learning algorithms marks a considerable improvement in the use of dynamic EEG analysis for SZ detection. The very high F1-score demonstrates the capability of computational methods to support psychiatric diagnostics, providing an objective and non-invasive instrument for early detection and intervention. This approach needs additional refinement and validation based on demographically and clinically broader dataset to verify its reliability and applicability.

Acknowledgments

We want to express our deep gratitude to the Neuroscience Research Center at Baqiyatallah University of Medical Sciences for their valuable support and resources that contributed significantly to the success of this study. We are extremely grateful to the Kaggle website for providing access to the data for the scientific community (https://www.kaggle.com/datasets/broach/ buttontone-sz).

Author contributions

SV wrote the Python code, conducted the analyses, interpreted the data,

prepared figures, and wrote the main manuscript; MC participated in data analysis, design of the study, interpretation, and writing of the manuscript; AM participated in the design of the study, dataset selection, interpretation, leadership, editing, and finalizing of the manuscript.

Ethical consideration

All methods and analyses were conducted in accordance with the relevant guidelines and regulations, and the study protocol was approved by the Research Ethics Committee of Baqiyatallah University of Medical Sciences (Ethics code: IR.BMSU.BAQ.REC.1403.147).

Funding sources

This research did not receive any specific grant from funding agencies in the public, commercial, or not-for-profit sectors.

Declaration of Competing Interest

All authors declared no potential conflicts of interest with respect to the research, authorship, and/or publication of this article.

Data availability

The dataset is publicly available on

Kaggle at: https://www.kaggle.com/datasets/broach/button-

tone-sz.

References

- (1) A. Mohammadi, V.G. Amooeian, E. Rashidi, Dysfunction in Brain-Derived Neurotrophic Factor Signaling Pathway and Susceptibility to Schizophrenia, Parkinson's and Alzheimer's Diseases, Curr Gene Ther 18 (2018). https://doi.org/10.2174/1566523218666180302163029.
- (2) James, S. L. et al. Global, regional, and national incidence, prevalence, and years lived with disability for 354 Diseases and Injuries for 195 countries and territories, 1990-2017: A systematic analysis for the Global Burden of Disease Study 2017. Lancet 392, 1789– 1858 (2018).
- C.U. Correll, B. Galling, A. Pawar, A. Krivko, C. Bonetto, M. Ruggeri, T.J. Craig, M. Nordentoft, V.H. Srihari, S. Guloksuz, C.L.M. Hui, E.Y.H. Chen, M. Valencia, F. Juarez, D.G. Robinson, N.R. Schooler, M.F. Brunette, K.T. Mueser, R.A. Rosenheck, P. Marcy, J. Addington, S.E. Estroff, J. Robinson, D. Penn, J.B. Severe, J.M. Kane, Comparison of Early Intervention Services vs Treatment as Usual for Early-Phase Psychosis: A Systematic Review, Meta-analysis, and Meta-regression, JAMA Psychiatry 75 (2018) 555–565. https://doi.org/10.1001/JAMAPSYCHIATRY.2018.0623.
- (4) J. Mcgrath, S. Saha, D. Chant, J. Welham, Schizophrenia: A Concise Overview of Incidence, Prevalence, and Mortality, (n.d.). https://doi.org/10.1093/epirev/mxn001.
- (5) A. Millier, U. Schmidt, M.C. Angermeyer, D. Chauhan, V. Murthy, M. Toumi, N. Cadi-Soussi, Humanistic burden in schizophrenia: A literature review, J Psychiatr Res 54 (2014) 85–93. https://doi.org/10.1016/J.JPSYCHIRES.2014.03.021.
- (6) E. Jääskeläinen, P. Juola, N. Hirvonen, J.J. McGrath, S. Saha, M. Isohanni, J. Veijola, J. Miettunen, A Systematic Review and Meta-Analysis of Recovery in Schizophrenia, Schizophr Bull 39 (2013) 1296–1306. https://doi.org/10.1093/SCHBUL/SBS130.
- (7) K. Hor, M. Taylor, Review: Suicide and schizophrenia: a systematic review of rates and risk factors, Journal of Psychopharmacology 24 (2010) 81–90. https://doi.org/10.1177/1359786810385490.
- (8) M. Nieuwenhuis, N.E.M. van Haren, H.E. Hulshoff Pol, W. Cahn, R.S. Kahn, H.G. Schnack, Classification of schizophrenia patients and healthy controls from structural MRI scans in two large independent samples, Neuroimage 61 (2012) 606–612. https://doi.org/10.1016/J.NEUROIMAGE.2012.03.079.
- (9) L. Orsolini, S. Pompili, U. Volpe, Schizophrenia: A Narrative Review of Etiopathogenetic, Diagnostic and Treatment Aspects, Journal of Clinical Medicine 2022, Vol. 11, Page 5040 11 (2022) 5040. https://doi.org/10.3390/JCM11175040.
- (10) A. Krauss, J. Bernard, O.O. Okusaga, Challenges and Considerations in Treating Negative and Cognitive Symptoms of Schizophrenia Spectrum Disorders, Federal Practitioner 39 (2022) 448. https://doi.org/10.12788/FP.0338.
- (11) M.W. Devries, P.A.E.G. Delespaul, Time, Context, and Subjective Experiences in Schizophrenia, Schizophr Bull 15 (1989) 233–244. https://doi.org/10.1093/SCHBUL/15.2.233.
- (12) T.H. McGlashan, Duration of untreated psychosis in first-episode schizophrenia: marker or determinant of course?, Biol Psychiatry 46 (1999) 899–907. https://doi.org/10.1016/S0006-3223(99)00084-0.
- (13) B. Narayanan, K. O'Neil, C. Berwise, M.C. Stevens, V.D. Calhoun, B.A. Clementz, C.A. Tamminga, J.A. Sweeney, M.S. Keshavan, G.D. Pearlson, Resting State Electroencephalogram Oscillatory Abnormalities in Schizophrenia and Psychotic Bipolar

- Patients and Their Relatives from the Bipolar and Schizophrenia Network on Intermediate Phenotypes Study, Biol Psychiatry 76 (2014) 456–465. https://doi.org/10.1016/J.BIOPSYCH.2013.12.008.
- (14) R. De Bock, A.J. Mackintosh, F. Maier, S. Borgwardt, A. Riecher-Rössler, C. Andreou, EEG microstates as biomarker for psychosis in ultra-high-risk patients, Transl Psychiatry 10 (2020) 300. https://doi.org/10.1038/s41398-020-00963-7.
- (15) T.G.L. Thaise Graziele, J.G.V. Miranda, R.S. do Rosário, E.P. de Sena, Brain instability in dynamic functional connectivity in schizophrenia, J Neural Transm 130 (2023) 171–180. https://doi.org/10.1007/S00702-022-02579-1/METRICS.
- (16) R. Aubonnet, M. HASSAN, P. Gargiulo, S. Seri, G. Di Lorenzo, Resting-State Electroencephalography Alpha Dynamic Connectivity: Quantifying Brain Network State Evolution in Individuals with Psychosis, (2024). https://doi.org/10.1101/2024.06.04.597416.
- (17) T.C. Yeh, C.C.Y. Huang, Y.A. Chung, S.Y. Park, J.J. Im, Y.Y. Lin, C.C. Ma, N.S. Tzeng, H.A. Chang, Resting-State EEG Connectivity at High-Frequency Bands and Attentional Performance Dysfunction in Stabilized Schizophrenia Patients, Medicina 2023, Vol. 59, Page 737 59 (2023) 737. https://doi.org/10.3390/MEDICINA59040737.
- (18) M. Cinelli, I. Echegoyen, M. Oliveira, S. Orellana, T. Gili, Altered Modularity and Disproportional Integration in Functional Networks are Markers of Abnormal Brain Organization in Schizophrenia, (2018). https://arxiv.org/abs/1805.04329v1 (accessed March 11, 2025).
- (19) D. Koshiyama, M. Miyakoshi, K. Tanaka-Koshiyama, Y.B. Joshi, J.L. Molina, J. Sprock, D.L. Braff, G.A. Light, Neurophysiologic Characterization of Resting State Connectivity Abnormalities in Schizophrenia Patients, Front Psychiatry 11 (2020) 608154. https://doi.org/10.3389/FPSYT.2020.608154/BIBTEX.
- (20) M. Rubinov, E. Bullmore, Schizophrenia and abnormal brain network hubs, Dialogues Clin Neurosci 15 (2013) 339–349. https://doi.org/10.31887/DCNS.2013.15.3/MRUBINOV.
- (21) S.A. Valizadeh, R. Riener, S. Elmer, L. Jäncke, Decrypting the electrophysiological individuality of the human brain: Identification of individuals based on resting-state EEG activity, Neuroimage 197 (2019) 470–481. https://doi.org/10.1016/j.neuroimage.2019.04.005.
- (22) A.C. Metting van Rijn, A. Peper, C.A. Grimbergen, High-quality recording of bioelectric events Part 1 Interference reduction, theory and practice, Med Biol Eng Comput 28 (1990) 389–397. https://doi.org/10.1007/BF02441961/METRICS.
- (23) J.M. Ford, V.A. Palzes, B.J. Roach, D.H. Mathalon, Did I Do That? Abnormal Predictive Processes in Schizophrenia When Button Pressing to Deliver a Tone, Schizophr Bull 40 (2014) 804–812. https://doi.org/10.1093/SCHBUL/SBT072.
- (24) A.P. Pinheiro, M. Schwartze, M. Amorim, R. Coentre, P. Levy, S.A. Kotz, Changes in motor preparation affect the sensory consequences of voice production in voice hearers, Neuropsychologia 146 (2020) 107531. https://doi.org/10.1016/J.NEUROPSYCHOLOGIA.2020.107531.
- (25) C. Barros, B. Roach, J.M. Ford, A.P. Pinheiro, C.A. Silva, From Sound Perception to Automatic Detection of Schizophrenia: An EEG-Based Deep Learning Approach, Front Psychiatry 12 (2022). https://doi.org/10.3389/FPSYT.2021.813460/FULL.

- J. Gao, D. Zhang, L. Wang, W. Wang, Y. Fan, M. Tang, X. Zhang, X. Lei, Y. Wang, J. Yang, X. Zhang, Altered Effective Connectivity in Schizophrenic Patients With Auditory Verbal Hallucinations: A Resting- State fMRI Study With Granger Causality Analysis, Front Psychiatry 11 (2020). https://doi.org/10.3389/FPSYT.2020.00575/FULL.
- (27) H. Huang, C. Shu, J. Chen, J. Zou, C. Chen, ... S.W.-P.R., undefined 2018, Altered corticostriatal pathway in first-episode paranoid schizophrenia: resting-state functional and causal connectivity analyses, Elsevier (n.d.). https://www.sciencedirect.com/science/article/pii/S0925492717300938 (accessed June 28, 2025).
- (28) T.K. Ho, The random subspace method for constructing decision forests, IEEE Trans Pattern Anal Mach Intell 20 (1998) 832–844. https://doi.org/10.1109/34.709601.
- (29) S.A. Valizadeh, F. Liem, S. Mérillat, J. Hänggi, L. Jäncke, Identification of individual subjects on the basis of their brain anatomical features, Sci Rep 8 (2018) 5611. https://doi.org/10.1038/s41598-018- 23696-6.
- (30) K. Fawagreh, M.M. Gaber, E. Elyan, Random forests: from early developments to recent advancements, Systems Science & Control Engineering: An Open Access Journal 2 (2014) 602–609. https://doi.org/10.1080/21642583.2014.956265.
- (31) H. Wang, F. Yang, Z. Luo, An experimental study of the intrinsic stability of random forest variable importance measures, BMC Bioinformatics 17 (2016) 1–18. https://doi.org/10.1186/S12859-016-0900- 5/FIGURES/9.
- (32) J. Luan, C. Zhang, B. Xu, Y. Xue, Y.R.-F. Research, undefined 2020, The predictive performances of random forest models with limited sample size and different species traits, ElsevierJ Luan, C Zhang, B Xu,
- (33) Xue, Y RenFisheries Research, 2020•Elsevier (n.d.). https://www.sciencedirect.com/science/article/pii/S0165783620300515 (accessed March 15, 2025).
- (34) H. Zhang, M.W.-S. and its Interface, undefined 2009, Search for the smallest random forest, Pmc.Ncbi.Nlm.Nih.GovH Zhang, M WangStatistics and Its Interface, 2009*pmc.Ncbi.Nlm.Nih.Gov (n.d.). https://pmc.ncbi.nlm.nih.gov/articles/PMC2822360/ (accessed March 15, 2025).
- (35) M. Becske, C. Marosi, H. Molnár, Z. Fodor, K. Farkas, F. Sámuel Rácz, M. Baradits, G. Csukly, Minimum spanning tree analysis of EEG resting-state functional networks in schizophrenia, Nature.ComM Becske, C Marosi, H Molnár, Z Fodor, K Farkas, FS Rácz, M Baradits, G CsuklyScientific Reports, 2024•nature.Com 14 (123AD) 10495. https://doi.org/10.1038/s41598-024-61316-8.
- (36) S. Mahato, L.K. Pathak, K. Kumari, Detection of Schizophrenia Using EEG Signals, Data Analytics in Bioinformatics:

 Learning Perspective (2021) 359–390. https://doi.org/10.1002/9781119785620.CH15.
- (37) Y. Hirano, I. Nakamura, S. Tamura, T. Onitsuka, Long-Term Test-Retest Reliability of Auditory Gamma Oscillations Between Different Clinical EEG Systems, Front Psychiatry 11 (2020). https://doi.org/10.3389/FPSYT.2020.00876/FULL.
- (38) A. Zeltser, A. Ochneva, ... D.R.-J. of C., undefined 2024, EEG Techniques with Brain Activity Localization, Specifically LORETA, and Its Applicability in Monitoring Schizophrenia, Mdpi.ComA Zeltser, A Ochneva, D Riabinina, V Zakurazhnaya, A Tsurina, E Golubeva, A BerdalinJournal of Clinical Medicine, 2024•mdpi.Com (n.d.). https://www.mdpi.com/2077-0383/13/17/5108 (accessed March 15, 2025).

- (39) N. Shaffi, M. Mahmud, F. Hajamohideen, K. Subramanian, M. Shamim Kaiser, Machine Learning and Deep Learning Methods for the Detection of Schizophrenia Using Magnetic Resonance Images and EEG Signals: An Overview of the Recent Advancements, Lecture Notes in Networks and Systems 623 LNNS (2023) 849–866. https://doi.org/10.1007/978-981-19-9638-2_72.
- (40) P. Rani, B.P.-A. Biophysics, undefined 2023, Multi-class EEG signal classification with statistical binary pattern synergic network for schizophrenia severity diagnosis., Aimspress.ComPE Rani, B PavanAIMS Biophysics, 2023*aimspress.Com 10 (2023) 347–371. https://doi.org/10.3934/biophy.2023021.
- (41) S. Srinivasan, S.J.-E.S. with Applications, undefined 2024, A novel approach to schizophrenia Detection: Optimized preprocessing and deep learning analysis of multichannel EEG data, ElsevierS Srinivasan, SD JohnsonExpert Systems with Applications, 2024•Elsevier (n.d.). https://www.sciencedirect.com/science/article/pii/S0957417423034395 (accessed June 28, 2025).
- (42) E. Paraschiv, L. Băjenaru, C. Petrache, O.B.-F. Internet, undefined 2024, Al-Driven Neuro-Monitoring: Advancing Schizophrenia Detection and Management Through Deep Learning and EEG Analysis, Mdpi.ComEA Paraschiv, L Băjenaru, C Petrache, O Bica, DN NicolauFuture Internet, 2024•mdpi.Com (n.d.). https://www.mdpi.com/1999-5903/16/11/424 (accessed June 28, 2025).
- (43) N. Swastika, Diagnosis for Schizophrenia Patients in EEG Signals Using Multiple Optimizers in Convolutional Neural Network (CNN), (2022). https://repository.i3l.ac.id/handle/123456789/741 (accessed June 28, 2025).
- (44) A. Rao, R. Ranjan, B. Sahana, G.K.-P. and Engineering, undefined 2025, SchizoLMNet: a modified lightweight MobileNetV2-architecture for automated schizophrenia detection using EEG-derived spectrograms, SpringerAP Rao, R Ranjan, BC Sahana, GP KumarPhysical and Engineering Sciences in Medicine, 2025•Springer (n.d.). https://link.springer.com/article/10.1007/s13246-024-01512-y (accessed June 28, 2025).
- (45)K. Stunnenberg, ... R.H.-I. 2024-2024, undefined 2024, Tensor Decomposition-Based Fusion for Biomarker Extraction from Multiple EEG Experiments, leeexplore.leee.OrgKR Stunnenberg, RC Hendriks, JL Vroegop, ML Adank, B HunyadilCASSP 2024-2024 IEEE International Conference Acoustics, 2024•ieeexplore.leee.Org (n.d.). https://ieeexplore.ieee.org/abstract/document/10448073/ (accessed June 28, 2025).
- (46) G. Sahu, M. Karnati, A. Gupta, A.S.-B.S.P. and, undefined 2023, SCZ-SCAN: An automated Schizophrenia detection system from electroencephalogram signals, ElsevierG Sahu, M Karnati, A Gupta, A SealBiomedical Signal Processing and Control, 2023 Elsevier (n.d.). https://www.sciencedirect.com/science/article/pii/S1746809423006390 (accessed June 28, 2025).
- H. Chen, Y. Lei, R. Li, X. Xia, N. Cui, X. Chen, ... J.L.-M., undefined 2024, Resting-state EEG dynamic functional connectivity distinguishes non-psychotic major depression, psychotic major depression and schizophrenia, Nature.ComH Chen, Y Lei, R Li, X Xia, N Cui, X Chen, J Liu, H Tang, J Zhou, Y Huang, Y Tian, X WangMolecular Psychiatry, 2024•nature.Com (n.d.). https://www.nature.com/articles/s41380- 023-02395-3 (accessed June 28, 2025).
- (48) M. Shen, P. Wen, B. Song, Y.L.-C. in B. and Medicine, undefined 2023, Automatic identification of schizophrenia based on EEG signals using dynamic functional connectivity analysis and 3D convolutional neural network, ElsevierM Shen, P Wen, B

- Song, Y LiComputers in Biology and Medicine, 2023•Elsevier (n.d.). https://www.sciencedirect.com/science/article/pii/S0010482523004870 (accessed June 28, 2025).
- (49) C. Ciprian, K. Masychev, M. Ravan, A. Manimaran, A. Deshmukh, Diagnosing schizophrenia using effective connectivity of resting-state EEG data, Algorithms 14 (2021) 139. https://doi.org/10.3390/a14050139.
- (50) A. Al Mazroa, M. Eltahir, S. Ebad, ... F.A.-P.C., undefined 2025, EEG-based schizophrenia diagnosis using deep learning with multi-scale and adaptive feature selection, Peerj.ComA Al Mazroa, MM Eltahir, SA Ebad, FA Alotaibi, J ChoPeerJ Computer Science, 2025•peerj.Com (n.d.). https://peerj.com/articles/cs-2811/(accessed June 28, 2025).
- (51) E. Castro, V. Gómez-Verdejo, M.M.-R.- Neurolmage, undefined 2014, A multiple kernel learning approach to perform classification of groups from complex-valued fMRI data analysis: application to schizophrenia, ElsevierE Castro, V Gómez-Verdejo, M Martínez-Ramón, KA Kiehl, VD CalhounNeurolmage,
- (52) 2014•Elsevier (n.d.). https://www.sciencedirect.com/science/article/pii/S1053811913010884 (accessed June 28, 2025).
- (53) S. Siuly, Y. Li, P. Wen, O.F. Alcin, SchizoGoogLeNet: The GoogLeNet-Based Deep Feature Extraction Design for Automatic Detection of Schizophrenia, Comput Intell Neurosci 2022 (2022). https://doi.org/10.1155/2022/1992596.

Accepied Manuscill